Iraqi Journal of Physics, 2023 *Vol. 21 No. 4, PP. 24-31*

https://doi.org/10.30723/ijp.v21i4.1147 *P-ISSN: 2070-4003*
E-ISSN: 2664-5548

Study of the Symmetry Energy and the Nuclear Equation of State for ^{13}O -^{13}B and ^{13}N-^{13}C Mirror Nuclei

Rana Haithem Harith[1a*] and Ban Sabah Hameed[1b]
[1]*Department of Physics, College of Science for Women, University of Baghdad, Baghdad, Iraq*
[b]E-mail: bansh_phy@csw.uobaghdad.edu.iq
[a*]Corresponding author: ranaithawii@gmail.com

Abstract

In parallel with the shell model using the harmonic oscillator's single-particle wave functions, the Hartree-Fock approximation was also used to calculate the neutron skin thickness, the mirror charge radii, and the differences in proton radii for ^{13}O-^{13}B and ^{13}N-^{13}C mirror nuclei. The calculations were done for both mirror nuclei in the psdpn model space. Depending on the type of potential used, the calculated values of skin thickness are affected. The symmetry energy and the symmetry energy's slope at nuclear saturation density were also determined, and the ratio of the density to the saturation density of nuclear matter and the symmetry energy has a nearly linear correlation. The mirror energy displacement was calculated, and the findings corresponded well with the available experimental data for the binding energies of the studied mirror nuclei. The measured values of the symmetry energy coefficient for the pair of mirror nuclei agreed with the computed ones, and this coefficient's value rises exponentially as the difference in charge radius increases.

Article Info.

Keywords:
Equation of State, Symmetry Energy, Mirror Charges Radii, Mirror Energy Displacement, Slope of the Symmetry Energy.

Article history:
Received: Jun. 14,2023
Revised: Sep. 12, 2023
Accepted: Sep. 28, 2023
Published: Dec. 01,2023

1. Introduction

In recent years, nuclear physicists have directed their efforts to measure one of the most fundamental properties of exotic atomic nuclei to measure and calculate the charge radius. Since the electric charge of a nucleus is established using electromagnetic interaction probes, the study of the charge radius is highly interesting since its determination is free from most nuclear physics uncertainty resulting from the strong interaction [1-8]. The nuclear equation of state (NEOS) has been applied for the isospin asymmetric material and is required to measure the charge radii in the mirror mass nuclei [9-17]. The charge radius has one determined by Brown [18-23], within an error of around 0.005 fm, which is the limit on L of the charge mirror radius, and the difference in charge radius, ΔR_{ch}, of the mirror pairs has a relationship to the derivative of the symmetry energy (L). Information on the energy required to increase the neutron richness of nuclear systems is encoded in the nuclear symmetry energy (E_{sym}). It is currently poorly understood, especially at supra-saturation densities, yet it has significant effects on nuclear structure, reactions, and neutron star features. Discoveries in astrophysics and nuclear tests on Earth have provided some limited constraints on its slope parameter L at the nuclear matter saturation density [24-27]. For the mirror pairs ^{36}Ca/^{36}S and ^{38}Ca/^{38}Ar, the instability's charge radii of ^{36,38}Ca nuclei were calculated by Brown et al., and this information was utilized to calculate the ΔR_{ch}. They concluded that the linked R_{ch} and the slope of the energy symmetry L at the nuclear saturation density were set as L = 5–70 MeV, which excludes a large portion of forecasting models for an equation of state [28, 29].

This study aims is to investigate the nuclear structure of ^{13}O -^{13}B and ^{13}N -^{13}C pairs mirror nuclei using the harmonic oscillator's single-particle wave functions. Hartree-Fock approximation was also employed to calculate the difference of proton radii between mirror nuclei (R_{mirr}), neutron skin thickness (R_{skin}) and mirror charges (R_{ch}^{mirr}) radii which are proportional to the derivative of the nuclear equation of state (NEOS) at saturation density with ρ_0 = 0.16 nucleons/fm^3. The symmetry energy (E_{sym}), the slope of the symmetry energy (L), and mirror displacement energy (MDE) were also calculated for each pair and compared with the available data.

2. The Theory

The radius of proton dispersion in a nucleus with (Z, N) should match the neutron distribution radius in mirror nuclei with (N, Z). The neutron skin thickness or R_{eskin} (Z, N), should then naturally reflect the discrepancy between mirror-nuclei proton radii, R_{mirr}(Z, N) [28].

$$\mathrm{R_{skin}(Z,N)} \equiv \mathrm{R_n(Z,N)} - \mathrm{R_p(Z,N)} \approx \mathrm{R_p(N,Z)} - \mathrm{R_p(Z,N)} \equiv \mathrm{R_{mirr}(Z,N)} \qquad (\mathbf{1})$$

where R_n and R_p are rms radius of neutrons and protons, respectively.

The difference in ΔR_{ch} of root-mean-square charge radii R_{ch} of the mirror nuclei is given by [14, 18, 29]:

$$\Delta \mathrm{R_{ch}} = \mathrm{R_{ch}(Z,N)} - \mathrm{R_{ch}(N,Z)} \qquad (\mathbf{2})$$

The symmetry energy at nuclear matter saturation density (ρ_0 = 0.16 nucleons/fm^3) is given by [30]:

$$E_{sym}\,(\rho) \approx 31.6\left(\frac{\rho}{\rho_\circ}\right)^{\gamma} \qquad (\mathbf{3})$$

where $\gamma = 0.69 - 1.05$ and ρ is the matter density.

The derivative symmetry energy is proportional with the neutron skins and given by [18, 31]:

$$\mathrm{L} = 3\rho\left[\frac{\partial \mathrm{E_{sym}}(\rho)}{\partial \rho}\right]\Big|_{\rho=\rho_\circ} \qquad (\mathbf{4})$$

L is crucial for applying the NEOS to lower and higher densities, which is necessary to comprehend the structure of mirror nuclei.

When Coulomb interaction is considered, the energy difference between two mirror nuclei is anticipated and it is a very obvious result of isospin symmetry-breaking, which is caused by the electromagnetic interaction. The difference between the binding energies (BE) of mirror nuclei is what is used to define the mirror displacement energy (MDE) [32, 33]:

$$\mathrm{MDE} = \mathrm{BE(T,T_z} = -\mathrm{T}) - \mathrm{BE(T\,,T_z} = +\mathrm{T}) \qquad (\mathbf{5})$$

3. Results and discussion

In this paper, the neutron skin thickness and the proton mirror of light mirror nuclei with mass number A=13 were calculated by computing the neutron and proton radii using the psdmod interaction [34, 35]. The Calculations were done in the psdpn model space by employing the shell model code Nushellx [36]. According to this interaction, the one-body matrix elements were calculated for two-particle interaction

with proton-proton and neutron-neutron pairs. The one-body potential was produced using SkXs25 parameterizations, adopting two single-particle-potential HO with a size parameter of b = 1.685 fm and HF approximation [37-39]. Proton-rich and neutron-rich nuclei are unstable (exotic) nuclei, which means their proton-to-neutron ratio is very different from the proton-to-neutron ratio in stable nuclei. An atomic nucleus with a protons-to-neutrons ratio significantly higher than those in stable nuclei is considered proton-rich. When it comes to the neutron-rich nucleus, it has a neutron skin and is referred to as such because the ratio of neutrons to protons is higher [40-42]. The Calculations R_{skin} of the used nuclei showed the distinction between the proton- and neutron-rich nuclei in the current study.

The R_{skin} is measured in fm units and equals to $R_{skin} = R_n - R_p$, when (R_n) and (R_p) are rms radius of neutrons and protons, respectively. For ^{13}O -^{13}B mirror nuclei, the R_{skin} of the ^{13}O nuclei is -0.083 when the HO potential is used, and -0.414 when using the HF potential. The negative values of R_{skin} are because the ^{13}O nucleus is a rich with proton. The R_{skin} for ^{13}B nucleus when using HO potential is 0.085, but when using the HF potential R_{skin} is 0.305. Similarly, for ^{13}N -^{13}C mirror nuclei, the R_{skin} of ^{13}N nucleus using the HO potential is -0.027, this value is close to R_{skin} value of ^{13}C nucleus but with the opposite sign, using the HF potential, the R_{skin} for ^{13}N nucleus is -0.169 but for ^{13}C nucleus is 0.084.

One can conclude that the values of R_{skin} it's varies according to the kind of potential used and the small difference in R_{skin} results between the two pairs mirror due to the kinetic energy operator difference between the proton and neutron masses. The Coulomb interaction pushes out the density of the protons relative to neutrons, causing an imbalance in the neutron skin. The calculated value of R_{mirr} and R_{ch}^{mirr} when using the HO wave function are less than when using the HF wave function for the same above reasons. For ^{13}O -^{13}B mirror nuclei, when the absolute value of $|N - Z|$ is equal to 3, the value of ΔR_{np} or ΔR_{skin} is 0.1095 fm, which is larger than that the value of ΔR_{np} for ^{13}N -^{13}C mirror nuclei and when the $|N - Z| = 1$ (small), the same results of calculated values of ΔR_{ch}^{mirr} are obtained. All results are shown in Table 1 and compared with experimental data [43].

Table 1: Calculated mirror, skin and mirror charges radii of ^{13}O-^{13}B and^{13}N-^{13}C using HO and HF eigen functions. The calculated R_{ch}^{mirr} are compared with the experimental data [43].

Nuclei	$J^{\pi}T$	HO eigen function			HF eigen function			R_{ch}^{mirr} Exp(fm)
		R_{ch}^{mirr}	R_{mirr}	R_{skin}	R_{ch}^{mirr}	R_{mirr}	R_{skin}	
^{13}O	$\frac{3}{2}^{-}\ \frac{3}{2}$	0.02	0.012	-0.083	0.392	0.398	-0.414	-------
^{13}B				0.085			0.305	
^{13}N	$\frac{1}{2}^{-}\ \frac{1}{2}$	0.022	0.027	-0.027	0.13	0.138	-0.169	0.0114
^{13}C				0.027			0.084	

Fig. 1 displays the outcomes of the neutron skins employing the HF potential of ^{13}B against the difference in mirror radius between the protons in ^{13}O and ^{13}B. The plot's points roughly follow a straight line except for higher R_{mirr}. This results from the self-consistent conflict between the symmetry potential and the Coulomb interaction in the calculations of the energy-density function.

Understanding the structure of nuclei requires an understanding of the density dependence of nuclear symmetry energy. Fig.2 displays the density dependence of E_{sym} for HF approximation using SkXs25 parameterizations. It is seen that the relationship of

symmetry energy with the ratio of density to saturation density of nuclear matter is almost a linear relationship.

In mirror nuclei, the NN interaction includes isospin-symmetry-breaking components, where the V_{nn} was found to be around 1% stronger than the pp interaction, V_{pp} and the np interaction, and V_{np} to be about 2.5% stronger than the average between V_{nn} and V_{pp}. Both of these effects are referred to as charge-independence breaking and charge-symmetry breaking, respectively [44]. Protons and neutrons have distinct masses, which result in various kinetic energies and affect the boson or two-boson exchange. This is where the charge-symmetry breaking force comes from. The pion mass splitting is the primary contributor to the charge-independence breaking force [45, 46]. The mirror displacement energy (MDE) is where the isospin-symmetry-breaking is most visibly present. The calculated MED for ^{13}O -^{13}B pair mirror nuclei is 9.6608 MeV which is agreed with the experimental value 8.90006 MeV [47]. For ^{13}N-^{13}C, the calculated value of 3.3 MeV is close to the experimental value. The values are shown in Table 2.

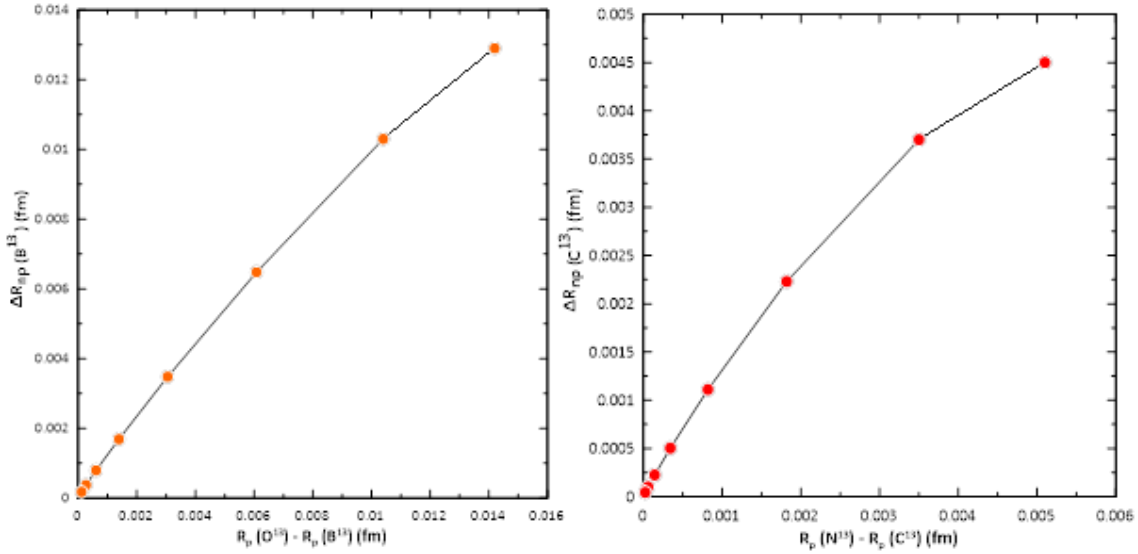

Figure 1: Relationship between the R_{mirr} of the mirror nuclei ^{13}O - ^{13}B and ^{13}N - ^{13}C with the R_{skin} of ^{13}B and ^{13}C, respectively.

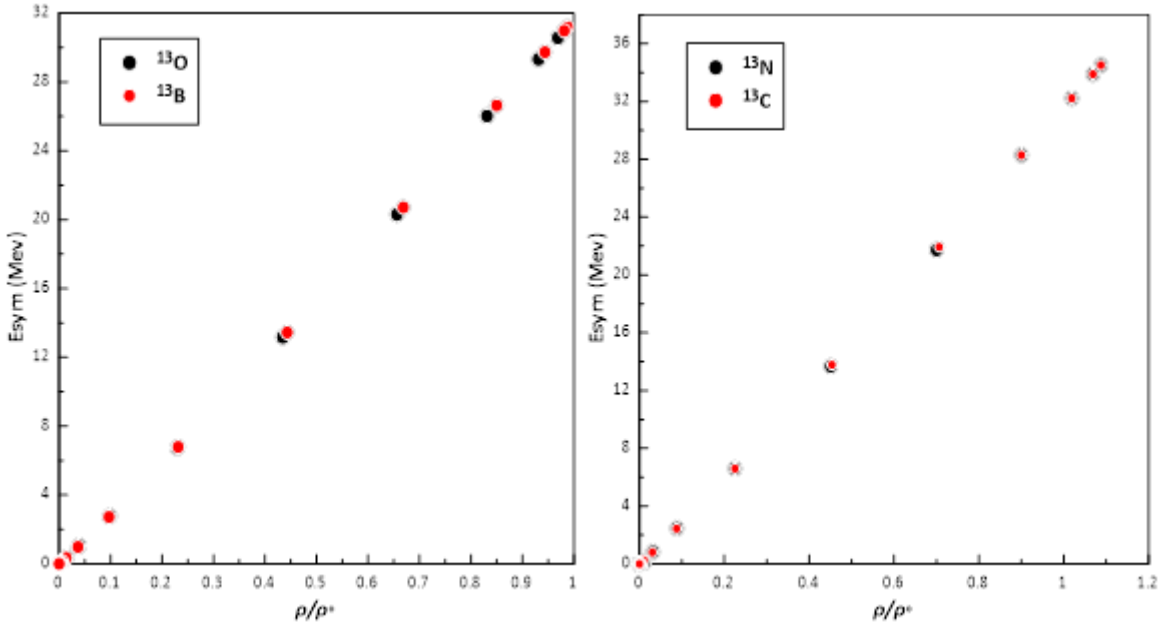

Figure 2: Relationship between the $\rho/\rho_{\circ}$ of the mirror nuclei ^{13}O - ^{13}B and ^{13}N - ^{13}C with the E_{sym}.

The calculated slope of the symmetry energy parameter L of ^{13}O -^{13}B and ^{13}N-^{13}C pair mirror nuclei are 114.67 and 114.43, respectively, which are agreed with the measured value 106±37 MeV [48]. The relationship between the L parameter and R_{skin} for the ^{13}O-^{13}B and ^{13}N-^{13}C pair mirror nuclei using HF potential is shown in Table 2 and Fig. 3. In the presence of Coulomb corrections, the difference in charge radius ΔR_{Ch} of the mirror nuclei is proportional to the parameter L at the saturation density [49]. It was noticed from Fig. 4 that the value of L increased exponentially with the increase of ΔR_{Ch} for both mirror nuclei. Nuclear matter's symmetry energy at saturation density and its entire density dependence have garnered much attention in recent years. The symmetry energy measures the system's binding change as the neutron-to-proton ratio changes at a fixed value of the total number of particles. As a result, it can be thought of as the symmetry energy as a function of density. It was shown that instability may occur for nuclear models with small values of symmetry energy.

The neutron skin R_{skin} or R_{np}, E_{sym} and R_{ch} depends on both $|N-Z| \times L$. The L dependency in R_{ski} predominates as $N-Z$ increases. Incorporating a surface symmetry energy factor into the nuclear mass formula, Brown [18, 50] has examined this dependency. The L factor is dominant when $|N-Z|$ is large. However, when $|N-Z|$drops to zero, just the E_{sym} factor is left.

***Table 2*: The calculated value of slope of the symmetry energy and the mirror displacement energy for ^{13}O -^{13}B and ^{13}N-^{13}C mirror nuclei.**

Mirror Nuclei	symmetry energy slope parameter (*L*) (MeV)	MED (Mev)	
	Cal.	Cal.	Exp
^{13}O -^{13}B	114.67	9.6608	8.90006
^{13}N-^{13}C	114.43	3.3	3.00283

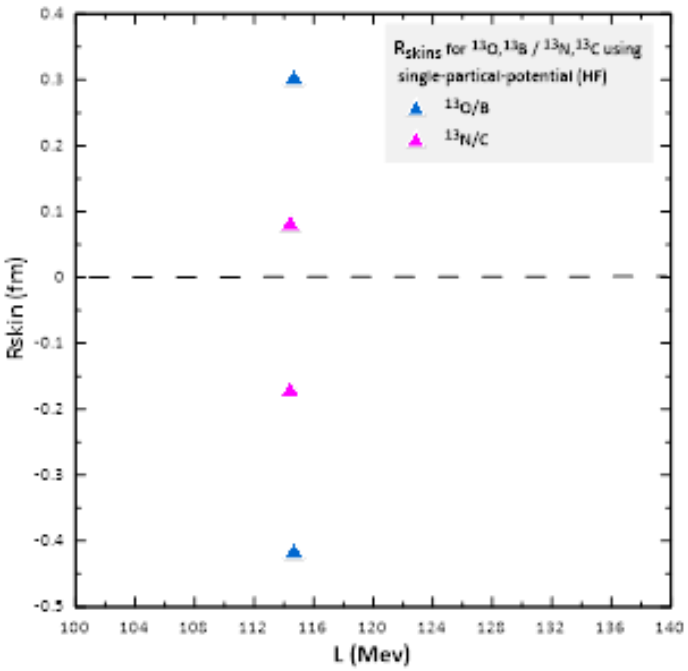

Figure 3: Represent the relationship between the L parameter and R_{skin} for the ^{13}O -^{13}B and ^{13}N-^{13}C pair mirror.

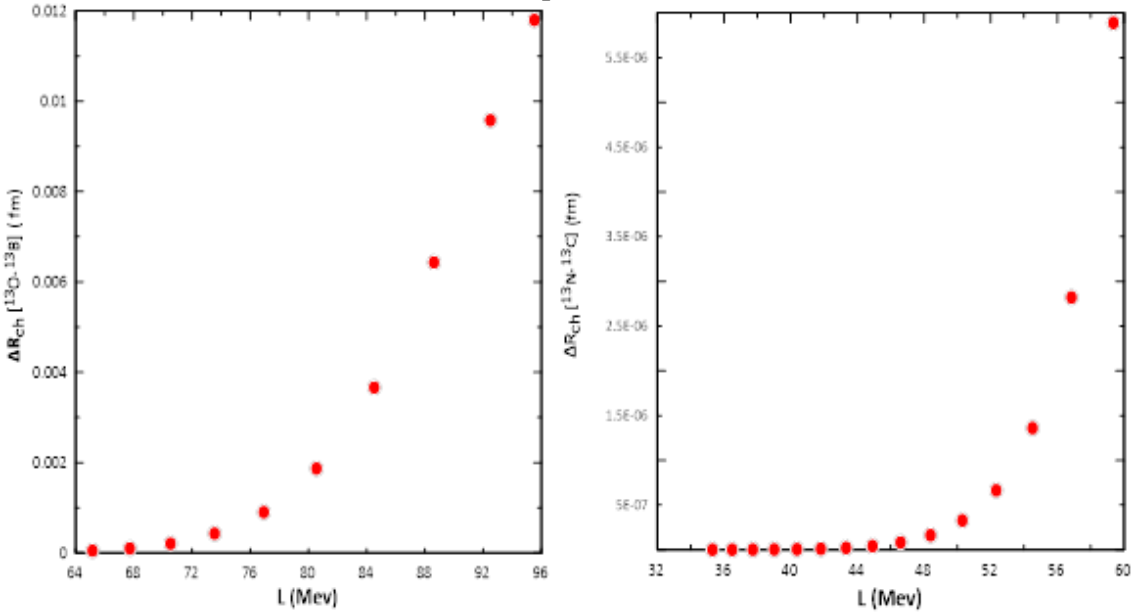

Figure 4: Relationship between the ΔR_{Ch} of the mirror nuclei ^{13}O - ^{13}B and ^{13}N - ^{13}C with the L.

4. Conclusions

The nuclear structure of ^{13}O-^{13}B and ^{13}N-^{13}C mirror nuclei is analyzed using HO and HF wave functions. Due to the kinetic energy operator difference between the proton and neutron masses, there was a slight discrepancy in R_{skin} findings between the two sets of mirrors. The values of R_{skin} were different according to the type of potential applied. When utilizing the HO wave function, R_{mirr} and R_{ch}^{mirr} were estimated at lower values than when using the HF wave function. The calculations of MDE were a good match with the data that is currently available for the mirror nuclei's different binding energies.

Lastly, the ratio of the density to saturation density of nuclear matter and the symmetry energy has a nearly linear correlation and the calculated value of slope of the

symmetry energy parameter L for the mirror nuclei pairs ^{13}O-^{13}B and ^{13}N-^{13}C was agreed with the measured value. The value of L was increased exponentially with the increase of ΔR_{Ch} for both mirror nuclei.

Acknowledgements

The authors would like to thank the University of Baghdad, Collage of Science for Women, Department of Physics, for assisting us in this article.

Conflict of Interest

The authors declare that they have no conflict of interest

References

1. B. S. Hameed and B. K. Rejah, Baghdad Sci. J. **19**, 1566 (2022).
2. B. S. Hameed and T. A. Alwan, Baghdad Sci. J. **20**, 0235 (2023).
3. S. K. Raheem, Z. Dakhil, and B. Hameed, in Journal of Physics: Conference Series (IOP Publishing, 2021). p. 012023.
4. B. S. Hameed, F. F. Kaddoori, and A. D. Salloum, Tre. Sci. **19**, 4169 (2022).
5. B. A. Brown, Nucl. Phys. A **704**, 11 (2002).
6. A. Ali and B. Hameed, Romanian J. Phys. **65**, 305 (2020).
7. L. Coraggio, G. De Gregorio, A. Gargano, N. Itaco, T. Fukui, Y. Ma, and F. Xu, Phys. Rev. C **102**, 054326 (2020).
8. B. S. Hameed, Int. J. Sci. Res. **6**, 2162 (2017).
9. R. A. Yajzey, PhD Thesis, University of York, 2021.
10. T. Naito, X. Roca-Maza, G. Colò, H. Liang, and H. Sagawa, Phys. Rev. C **106**, L061306 (2022).
11. K. Kaneko, S. Tazaki, T. Mizusaki, Y. Sun, M. Hasegawa, and G. De Angelis, Phys. Rev. C **82**, 061301 (2010).
12. S. Lenzi, A. Poves, and A. Macchiavelli, Phys. Rev. C **102**, 031302 (2020).
13. T. Naito, G. Colò, H. Liang, X. Roca-Maza, and H. Sagawa, Phys. Rev. C **105**, L021304 (2022).
14. T. Naito, G. Colò, H. Liang, X. Roca-Maza, and H. Sagawa, Phys. Rev. C **107**, 064302 (2023).
15. R. Wiringa, S. Pastore, S. C. Pieper, and G. A. Miller, Phys. Rev. C **88**, 044333 (2013).
16. P. Campbell, I. Moore, and M. Pearson, Prog. Part. Nucl. Phys. **86**, 127 (2016).
17. T. Suda and H. Simon, Prog. Part. Nucl. Phys. **96**, 1 (2017).
18. B. A. Brown, Phys. Rev. Lett. **119**, 122502 (2017).
19. B. A. Brown, Phys. Rev. Lett. **111**, 232502 (2013).
20. S. Typel and B. A. Brown, Phys. Rev. C **64**, 027302 (2001).
21. B. Hu, W. Jiang, T. Miyagi, Z. Sun, A. Ekström, C. Forssén, G. Hagen, J. D. Holt, T. Papenbrock, and S. R. Stroberg, Nat. Phys. **18**, 1196 (2022).
22. Y. Huang, Z. Li, and Y. Niu, Phys. Rev. C **107**, 034319 (2023).
23. B.-A. Li and M. Magno, Phys. Rev. C **102**, 045807 (2020).
24. B.-A. Li and X. Han, Phys. Lett. B **727**, 276 (2013).
25. P. Bano, S. Pattnaik, M. Centelles, X. Viñas, and T. Routray, Phys. Rev. C **108**, 015802 (2023).
26. B. Brown, K. Minamisono, J. Piekarewicz, H. Hergert, D. Garand, A. Klose, K. König, J. Lantis, Y. Liu, and B. Maaß, Phys. Rev. Res. **2**, 022035 (2020).
27. J. Yang and J. Piekarewicz, Phys. Rev. C **97**, 014314 (2018).
28. J.-Y. Xu, Z.-Z. Li, B.-H. Sun, Y.-F. Niu, X. Roca-Maza, H. Sagawa, and I. Tanihata, Phys. Lett. B **833**, 137333 (2022).

29. K. König, J. C. Berengut, A. Borschevsky, A. Brinson, B. A. Brown, A. Dockery, S. Elhatisari, E. Eliav, R. F. G. Ruiz, J. D. Holt, B.-S. Hu, J. Karthein, D. Lee, Y.-Z. Ma, U.-G. Meißner, K. Minamisono, A. V. Oleynichenko, S. Pineda, S. D. Prosnyak, M. L. Reitsma, L. V. Skripnikov, A. Vernon, and A. Zaitsevski, Nucl. Exper. **2023**, (2023).
30. L.-W. Chen, C. M. Ko, and B.-A. Li, Phys. Rev. Lett. **94**, 032701 (2005).
31. J. Lattimer and M. Prakash, Astrophys. J. **550**, 426 (2001).
32. P. Bączyk, J. Dobaczewski, M. Konieczka, W. Satuła, T. Nakatsukasa, and K. Sato, Phys. Lett. B **778**, 178 (2018).
33. J. Nolen Jr and J. Schiffer, Ann. Rev. Nucl. Sci. **19**, 471 (1969).
34. Y. Utsuno and S. Chiba, Phys. Rev. C **83**, 021301 (2011).
35. R. Meharchand, R. Zegers, B. Brown, S. M. Austin, T. Baugher, D. Bazin, J. Deaven, A. Gade, G. Grinyer, and C. Guess, Phys. Rev. Lett. **108**, 122501 (2012).
36. B. Brown and W. Rae, Nucl. Dat. Sheets **120**, 115 (2014).
37. C. Tsang, B. Brown, F. Fattoyev, W. Lynch, and M. Tsang, Phys. Rev. C **100**, 062801 (2019).
38. A. Tichai, J. Müller, K. Vobig, and R. Roth, Phys. Rev. C **99**, 034321 (2019).
39. S. J. Novario, G. Hagen, G. R. Jansen, and T. Papenbrock, Phys. Rev. C **102**, 051303 (2020).
40. S. G. Zhou, in Proceedings of The 26th International Nuclear Physics Conference (Adelaide, Australia Proceedings of Science, 2016). p. 373.
41. P. Punta, J. A. Lay, and A. M. Moro, Phys. Rev. C **108**, 024613 (2023).
42. A. a. M. Hussein and G. N. Flaiyh, E. Eur. J. Phys., 75 (2023).
43. I. Angeli and K. P. Marinova, Atom. Dat. Nucl. Dat. Tab. **99**, 69 (2013).
44. R. Machleidt, Phys. Rev. C **63**, 024001 (2001).
45. P. Bączyk, J. Dobaczewski, M. Konieczka, W. Satuła, T. Nakatsukasa, and K. Sato, Phys. Lett. B **778**, 178 (2018).
46. N. A. Smirnova, Physics **5**, 352 (2023).
47. X. Roca-Maza and N. Paar, Prog. Part. Nucl. Phy. **101**, 96 (2018).
48. B. T. Reed, F. J. Fattoyev, C. J. Horowitz, and J. Piekarewicz, Phys. Rev.Lett. **126**, 172503 (2021).
49. M. K. Gaidarov, I. Moumene, A. N. Antonov, D. N. Kadrev, P. Sarriguren, and E. Moya De Guerra, Nucl. Phys. A **1004**, 122061 (2020).
50. P. Danielewicz, Nucl. Phys. A **727**, 233 (2003).

دراسة طاقة التناظر ومعادلة الحالة النووية للنوى المرآتية ^{13}B- ^{13}O و^{13}C-^{13}N

رنا هيثم حارث[1] و بان صباح حميد[1]

[1] قسم الفيزياء، كلية العلوم للبنات، جامعة بغداد، بغداد، العراق

الخلاصة

وفقًا لنموذج القشرة، وباستخدام دوال موجة الجسيمات المفردة للمتذبذب التوافقي، وباستخدام تقريب هاتري- فوك أيضًا تم حساب أنصاف الاقطار لسمك القشرة النيوتروني والشحنة المرآتية وكذلك تم حساب الفرق بين أنصاف الاقطار لزوج النوى المرآتية ^{13}B-^{13}O و ^{13}C-^{13}N. تم إجراء الحسابات لكل من نوى المرآتية المذكورة أعلاه في مساحة نموذج psdpn. استنتجنا أن قيمة سمك القشرة يختلف اعتمادًا على نوع الجهود المستخدمة. تم أيضًا تحديد طاقة التناظر وانحدار طاقة التناظرعند كثافة التشبع النووي وكانت نسبة الكثافة الى كثافة التشبع للمادة النووية وطاقة التناظر لها علاقة خطية تقريبا. تم ايضا حساب إزاحة طاقة النوى المرآتية حيث اتفقت النتائج بشكل جيد مع البيانات التجريبية المتاحة لطاقات ربط نوى المرآتية المدروسة. أتفقت القيم المقاسة والمحسوبة لمعامل طاقة التماثل لزوج النوى المرآتية، وترتفع قيمة هذا المعامل اسياً مع زيادة الفرق في نصف قطر الشحنة.

الكلمات المفتاحية: معادلة الحالة، طاقة التناظر، نصف قطر الشحنة المرآتية، إزاحة الطاقة المرآتية، منحدر طاقة التناظر.